DMD Fast Forward. Published on April 25, 2016 as DOI: 10.1124/dmd.116.069575
This article has not been copyedited and formatted. The final version may differ from this version.

DMD # 69575

Zomepirac Acyl Glucuronide Is Responsible for Zomepirac-induced Acute Kidney Injury in Mice

Atsushi Iwamura, Katsuhito Watanabe, Sho Akai, Tsubasa Nishinosono, Koichi Tsuneyama, Shingo Oda, Toshiyuki Kume, and Tsuyoshi Yokoi

DMPK Research Laboratory, Mitsubishi Tanabe Pharma Corporation, Saitama, Japan (A.I., T.K.); Department of Drug Safety Sciences, Nagoya University Graduate School of Medicine, Aichi, Japan (K.W., S.A., T.N., S.O., T.Y.); Department of Molecular and Environmental Pathology, Institute of Health Biosciences Tokushima University Graduate School, Tokushima, Japan (K.T), and Drug Metabolism and Toxicology, Faculty of Pharmaceutical Sciences, Kanazawa University, Ishikawa, Japan (A.I.)

DMD Fast Forward. Published on April 25, 2016 as DOI: 10.1124/dmd.116.069575
This article has not been copyedited and formatted. The final version may differ from this version.

DMD # 69575

Running title: Kidney injury induced by zomepirac acyl glucuronide

Address correspondence to:

Atsushi Iwamura

DMPK Research Laboratory, Mitsubishi Tanabe Pharma Corporation, 2-2-50

Kawagishi, Toda, Saitama 335-8505, Japan.

Phone: +81-48-433-8419

Fax: +81-48-433-8170

E-mail: Iwamura.Atsushi@mf.mt-pharma.co.jp

Number of text pages: 44

Number of tables: 1

Number of figures: 8

Number of references: 52

Number of words in the Abstract: 249

Number of words in the Introduction: 574

Number of words in the Discussion: 1471

ABBREVIATIONS: AG, acyl glucuronide; ALT, alanine aminotransferase; BUN, blood urea nitrogen; BSO, L-buthionine-(*S*,*R*)-sulfoximine; CRE, creatinine; GAPDH,

glyceraldehyde-3-phosphate dehydrogenase; GSH, glutathione; GSSG, disulfide glutathione; HO-1, heme oxygenase 1; HPLC, high-performance liquid chromatography; ICAM-1, intercellular adhesion molecule-1; IL-1α, interleukin 1 alpha; IL-6, interleukin 6; IL-8, interleukin 8; KPB, potassium phosphate buffer; MDA, malondialdehyde; MIP-2, macrophage inflammatory protein-2; PBMCs, peripheral blood mononuclear cells; S100A9, S100 calcium-binding protein A9; TBARS, thiobarbituric acid reactive substances; TOTP, tri-*o*-tolyl phosphate; UDPGA, UDP-glucuronic acid; UGT, UDP-glucuronosyltransferase; ZP, zomepirac

Abstract

Glucuronidation, an important phase II metabolic route, is generally considered to be a detoxification pathway. However, acyl glucuronides (AGs) have been implicated in the toxicity of carboxylic acid drugs due to their electrophilic reactivity. Zomepirac (ZP) was withdrawn from the market because of adverse effects such as renal toxicity. Although ZP is mainly metabolized to acyl glucuronide (ZP-AG) by UDP-glucuronosyltransferase, the role of ZP-AG in renal toxicity is unknown. In this study, we established a ZP-induced kidney injury mouse model by pretreatment with tri-*o*-tolyl phosphate (TOTP), a non-selective esterase inhibitor, and L-buthionine-(*S*,*R*)-sulfoximine (BSO), a glutathione synthesis inhibitor. The role of ZP-AG in renal toxicity was investigated using this model. The model showed significant increases in blood urea nitrogen (BUN) and creatinine (CRE), but not alanine aminotransferase. The ZP-AG concentrations were elevated by co-treatment with TOTP in the plasma and liver and especially in the kidney. The ZP-AG concentrations in the kidney correlated with values for BUN and CRE. Upon histopathological examination, vacuoles and infiltration of mononuclear cells were observed in the model mouse. In addition to immune-related responses, oxidative stress

DMD Fast Forward. Published on April 25, 2016 as DOI: 10.1124/dmd.116.069575
This article has not been copyedited and formatted. The final version may differ from this version.

markers such as the glutathione/disulfide glutathione ratio and malondialdehyde levels were different in the mouse model. The suppression of ZP-induced kidney injury by tempol, an antioxidant agent, suggested the involvement of oxidative stress in ZP-induced kidney injury. This is the first study to demonstrate that AG accumulation in the kidney by TOTP and BSO treatment could explain renal toxicity and to show the *in vivo* toxicological potential of AGs.

DMD Fast Forward. Published on April 25, 2016 as DOI: 10.1124/dmd.116.069575
This article has not been copyedited and formatted. The final version may differ from this version.

Introduction

Acyl glucuronidation is one of the major metabolic routes of carboxylic acid-containing drugs. Glucuronidation is an important phase II metabolic pathway for endogenous and exogenous substrates and is generally considered as a detoxification pathway. However, acyl glucuronides (AGs) are unstable under physiological conditions and consequently undergo hydrolysis or intramolecular rearrangement through the migration of the drug moiety from the 1-*O*-position to the 2-, 3-, or 4-position on the glucuronic acid ring (Smith et al., 1990a; Benet et al., 1993; Bailey and Dickinson, 2003). Because of their electrophilic nature and ability to cause substitution reactions with nucleophilic groups in proteins or other macromolecules, AGs can covalently modify endogenous proteins and have been postulated to cause the adverse toxicity associated with carboxylic acid-containing drugs (Faed, 1984; Boelsterli, 2002). To assess the toxicity of AGs, several *in vitro* assay systems, such as stability assay by measuring half-lives in potassium phosphate buffer, peptide adducts assay and immunostimulation assay, have been proposed (Wang et al., 2004; Sawamura et al., 2010; Jinno et al., 2013; Miyashita et al., 2014; Iwamura et al., 2015). However, the toxicity of AGs has remained controversial because direct evidence of *in vivo* AGs

toxicity has not been provided.

Zomepirac (ZP), a nonsteroidal anti-inflammatory drug, was withdrawn from the market because of adverse effects such as anaphylaxis and renal toxicity (Smith, 1982; Miller et al., 1983; Heintz, 1995). ZP is mainly metabolized to acyl glucuronide (ZP-AG) in humans (Grindel et al., 1980; O'Neill et al., 1982). ZP-AG is more physicochemically unstable in phosphate buffer than the AGs of safe drugs such as gemfibrozil, repaglunide and telmisartan (Sawamura et al., 2010). ZP-AG also covalently modifies dipeptidyl peptidase IV in rat liver homogenates and microtubular protein in the bovine brain *in vitro* (Bailey et al., 1998; Wang et al., 2001). We previously demonstrated that ZP-AG showed the highest induction of the mRNA expression of immune- and inflammation-related genes in human peripheral blood mononuclear cells (PBMCs) in the AGs of 13 drugs (Iwamura et al., 2015). Although the toxicity of ZP-AG has been suggested, there is no evidence that ZP-AG is involved in ZP-induced toxicity *in vivo* in humans or laboratory animals because of the difficulty of toxicological assessment under the conditions required for sufficient exposure to ZP-AG *in vivo*.

The level of AG production is determined by glucuronidation catalyzed by UGT and enzymatic hydrolysis. The enzymatic hydrolysis of AG is catalyzed by esterases

such as acylpeptide hydrolase and α/β hydrolase domain containing (ABHD) 10 (Suzuki et al., 2010; Iwamura et al., 2012). It was reported that the plasma clearance of ZP-AG in the guinea pig was decreased by phenylmethylsulfonyl fluoride, a general esterase inhibitor, suggesting that ZP-AG is hydrolyzed by esterases (Smith et al., 1990b). In other reports, esterases were potently inhibited by tri-*o*-tolyl phosphate (TOTP), a non-selective esterase inhibitor, in mice and rats *in vivo* (Silver and Murphy, 1981; Kobayashi et al., 2012). ZP-AG conjugates with glutathione (GSH) in rat hepatocytes and bile (Grillo and Hua, 2003). Therefore, the ZP-AG level is regulated via hydrolysis by esterases and GSH conjugation against the generation by UGT. It is assumed that the increased exposure to ZP-AG *in vivo* by TOTP and L-buthionine-(*S*,*R*)-sulfoximine (BSO), a glutathione synthesis inhibitor, after ZP administration may show that ZP-AG rather than ZP is involved in ZP-induced toxicity *in vivo*. The purpose of the present study was to establish the ZP-induced kidney injury mouse model and to investigate the role of ZP-AG in kidney injury.

DMD Fast Forward. Published on April 25, 2016 as DOI: 10.1124/dmd.116.069575
This article has not been copyedited and formatted. The final version may differ from this version.

Materials and Methods

Chemicals and Reagents. Reduced GSH, oxidized GSH and BSO were purchased from Wako Pure Chemical Industries (Osaka, Japan). Zomepirac sodium and 4-hydroxy-2,2,6,6-tetramethylpiperidine 1-oxyl (tempol) were obtained from Sigma-Aldrich (St. Louis, MO). ZP-AG and TOTP was purchased from Toronto Research Chemicals (Ontario, Canada) and Acros Organics (Morris Plains, NJ), respectively. β-NADPH and GSH reductase were obtained from Oriental Yeast (Tokyo, Japan). A ReverTra Ace qPCR RT kit was obtained from Toyobo (Osaka, Japan). RNAiso Plus and SYBR Premix ExTaq (Tli RNaseH Plus) were obtained from Takara (Otsu, Japan). All primers were commercially synthesized at Hokkaido System Sciences (Sapporo, Japan). Fuji DRI-CHEM slides of GPT/ALT-PIII, BUN-PIII and CRE-PIII, which were used to measure alanine aminotransferase (ALT), blood urea nitrogen (BUN) and creatinine (CRE), respectively, were from Fujifilm (Tokyo, Japan). Rabbit polyclonal antibody against myeloperoxidase (MPO) was purchased from DAKO (Carpinteria, CA). A Thiobarbituric Acid Reactive Substances (TBARS) Assay kit was obtained from Oxford Biomedical Research (Oxford, MI). Other chemicals used in this study were of analytical grade or were the highest grade commercially available.

Animals. Nine- to eleven-week-old female BALB/cCrSlc mice were obtained from Japan SLC (Hamamatsu, Japan). The animals were housed under a 12-h light/dark cycle (lights on 9:00–21:00 hours) in a controlled environment (temperature 23 ± 2°C and humidity 55 ± 10%) in the institutional animal facility. All animals were allowed free access to food and water, except when fasting was being conducted. The animals were acclimatized before use in the experiments. All procedures were carried out in accordance with the guidelines established by the Institute for Laboratory Animal Research of the Medical School of Nagoya University.

Administration of ZP, TOTP and BSO. ZP was dissolved in potassium phosphate buffer (KPB, pH 7.4, 5-15 mg/mL) and intraperitoneally administered to the mice at a dose of 50-150 mg/kg. TOTP was dissolved in corn oil (10 mg/mL) and orally administered at a dose of 50 mg/kg to mice 12 h before ZP administration. BSO was dissolved in saline (70 mg/mL) and intraperitoneally administered at a dose of 700 mg/kg to mice 1 h before ZP administration after overnight fasting. The BSO dosage was confirmed at 700 mg/kg because a decreased hepatic GSH level was previously reported at this dose (Shimizu et al., 2009).

Administration of Antioxidant Agent. Mice were intraperitioneally administered

tempol, an antioxidant agent (200 mg/kg in sterilized PBS) at 6 h and 18 h after ZP administration. The plasma was collected at 12 h and 24 h after ZP administration.

Concentrations of ZP and ZP-AG in Plasma, Liver and Kidney. Plasma was obtained from heparinized blood by centrifugation at 13,000 *g* for 5 min at 4°C, and tissues were frozen by liquid nitrogen immediately after collection. Plasma and tissues were stored at -80°C prior to analysis. Mice livers and kidneys were quickly homogenized in homogenate buffer (10 mM Tris-HCl (pH 7.4), 20% glycerol, 1 mM EDTA (pH 8.0)) on ice. Plasma and tissue concentrations of ZP and ZP-AG were determined by high-performance liquid chromatography (HPLC) according to previous study (Smith et al., 1985a) with slight modifications. Briefly, 5 μL of plasma or 1.25 mg of tissue homogenates were mixed with 20 μL acetonitrile and 35 μL of 8% $HClO_4$ to precipitate the protein. Smith et al. (1985a) previously demonstrated that adding acids and organic solvents stabilized ZP-AG. The mixture was centrifuged at 13,000 *g* for 5 min, and a 40 μL sample of the supernatant was subjected to HPLC. The HPLC analysis was performed using an L-2130 pump (Hitachi), an L-2200 autosampler (Hitachi), and an L-2400 UV detector (Hitachi) equipped with a Mightysil RP-18 C18 GP column (5 μm particle size, 4.6 mm i.d. x 150 mm: Kanto Chemical, Tokyo, Japan). The eluent was monitored at 313 nm. The mobile phases were 47% methanol/10 mM acetate buffer

(pH 5.0). The quantification of ZP and ZP-AG was performed by comparing the HPLC peak areas with those of authentic standards. Standard samples were prepared in blank plasma and tissue homogenates for ZP and ZP-AG. In the preliminary study, it was confirmed that blank plasma and tissue homogenates did not affect standard curves of ZP and ZP-AG when standards were taken though the same steps as measured samples.

Histopathological Examination. Kidney samples were fixed in 10% neutral-buffered formalin. The fixed samples were dehydrated with alcohols and embedded in paraffin. Serial sections were stained with hematoxylin-eosin (H&E) for histopathological examination. Neutrophil infiltration was assessed by MPO immunostaining. A rabbit polyclonal antibody against MPO was used for kidney immunohistochemical staining, as previously described (Kumada et al., 2004). Two visual fields at a 200-fold magnification (0.2 mm^2 each) were randomly selected from each MPO-immunostained specimen. The average number of MPO-positive cells from two randomly selected visual fields was compared between the specimens.

Real-Time Reverse Transcription (RT)-Polymerase Chain Reaction (PCR). The RNA from mice livers and kidneys was isolated using RNAiso Plus according to the manufacturer's instructions. The mRNA expression of IL-1α, IL-6, macrophage inflammatory protein-2 (MIP-2/CXCL2), intercellular adhesion molecule-1

(ICAM-1/CD54), S100 calcium-binding protein A9 (S100A9), and heme oxygenase 1 (HO-1) were quantified using real-time RT-PCR. RT was performed using a ReverTra Ace qRT-PCR kit, according to the manufacturer's instructions. In brief, 1 μg of total RNA was mixed with an appropriate volume of five-fold RT buffer, enzyme mix, primer mix, and nuclease-free water to adjust the total volume to 20 μl, and the RT reaction was carried out at 37°C for 15 min and 98°C for 5 min. Real-time RT-PCR was performed using a Mx3000P (Agilent Technologies, Santa Clara, CA), and the PCR conditions included denaturation at 95°C for 30 s, followed by 40 amplification cycles of 95°C for 5 s and 60°C for all targets. The amplified products were monitored directly by measuring the increase in the intensity of the SYBR Green I dye binding to the double-stranded DNA amplified by PCR, and a dissociation curve analysis was conducted to confirm the amplification of the PCR product. The primer sequences used in this study are shown in Table 1.

Renal and Hepatic GSH Levels. Mice livers and kidneys were homogenized in ice-cold 5% sulfosalicylic acid and centrifuged at 8,000 *g* for 10 min at 4°C. The supernatant was collected, and the total GSH and disulfide glutathione (GSSG) concentrations were measured as previously described (Tietze, 1969; Griffith, 1980). The reduced GSH contents were calculated from the total GSH and GSSG contents.

Renal and Hepatic Malondialdehyde (MDA) Levels. Mice livers and kidneys were homogenized in homogenate buffer. A half volume of trichloroacetic acid (1 g/mL) was added to tissue homogenates to precipitate proteins and acidify the samples. The samples were then centrifuged at 12,000 *g* for 5 min at 4°C. The supernatant was collected, and the MDA concentrations were measured using a TBARS Assay kit (Oxford Biomedical Research) according to the manufacturer's protocol. The TBARS were detected by fluorescence (excitation 532 nm, emission 585 nm) using a PowerScan4 (DS Pharma Biomedical, Osaka, Japan).

Statistical Analysis. The statistical analysis of multiple groups was performed using Dunnett's test or Tukey's test to determine the significance of differences between individual groups. Comparisons between two groups were carried out using two-tailed Student's *t*-tests. A value of $P < 0.05$ was considered statistically significant.

DMD Fast Forward. Published on April 25, 2016 as DOI: 10.1124/dmd.116.069575
This article has not been copyedited and formatted. The final version may differ from this version.

Results

Establishment of the ZP-induced Kidney Injury Mouse Model. In female BALB/c mice treated with ZP alone, the plasma levels of CRE, BUN and ALT were not increased at 24 h after ZP administration (Fig. 1). Considering the possibility that GSH conjugation and hydrolysis of ZP-AG might be involved in ZP-induced toxicity, the effects of co-treatment with BSO or TOTP, a GSH synthesis inhibitor (Shimizu et al., 2009) or an esterase inhibitor (Emeigh Hart et al., 1991), respectively, were investigated. Co-administration of BSO resulted in a slight increase in CRE and BUN (0.640 and 94.5 mg/dL, respectively) compared to the group treated with ZP alone (0.340 and 50.6 mg/dL, respectively). However, CRE and BUN were significantly elevated by co-administration of TOTP (1.08 and 160 mg/dL, respectively), although ALT was not affected. The highest increases of CRE and BUN were observed in mice co-treated with both TOTP and BSO (1.49 and 176 mg/dL, respectively). No increase in plasma CRE, BUN and ALT levels in mice receiving TOTP or BSO only was confirmed. These results suggest that the inhibition of GSH conjugation and hydrolysis of ZP-AG contributes to the kidney injury caused by ZP administration.

Dose- and Time-dependent Changes in ZP-induced Kidney Injury. ZP was administered to mice at a dose of 50, 100, or 150 mg/kg with co-administration of TOTP and BSO. Plasma CRE and BUN levels were significantly and dose-dependently increased in mice receiving 100 (1.12 and 137 mg/dL, respectively) and 150 mg/kg (1.43 and 155 mg/dL, respectively) of ZP compared with vehicle (KPB)-treated control mice; thus, for subsequent experiments we adopted a dose of ZP at 150 mg/kg (Fig. 2). As shown in Figs. 3A-3C, plasma CRE and BUN levels were time-dependently increased 12 h (0.583 and 99.7 mg/dL, respectively) and 24 h (1.15 and 158 mg/dL, respectively) after ZP-administration, but plasma ALT levels were not.

Time-dependent Changes in ZP and ZP-AG Concentration in Plasma, Kidney and Liver. The concentrations of ZP and ZP-AG in plasma, kidney and liver were measured in mice after ZP administration with or without co-administration of TOTP and BSO. In plasma, kidney and liver, the concentrations of ZP were significantly lower in mice receiving TOTP, BSO and ZP compared to those in mice receiving ZP alone (Fig. 3D). However, the plasma and the tissue concentrations of ZP-AG were significantly higher in the mice receiving TOTP, BSO and ZP compared to mice receiving ZP alone (Fig. 3E). By co-administration with inhibitors, increases of 4.9-, 1.9- and 9.0-fold in the maximum concentration (Cmax) of ZP-AG were observed in

plasma, liver and kidney, respectively. The plasma Cmax of ZP-AG in mice receiving ZP and inhibitors was approximately 50-fold higher than those in humans after 100 mg oral dose of zomepirac (Smith et al., 1985b). In groups co-administered with or without the inhibitors, the ZP concentrations in the kidney were almost the same as those in the liver, whereas the ZP-AG concentrations in the kidney were much higher than those in the liver. These results imply that the ZP-AG is slowly eliminated from the kidney, resulting in a high accumulation in the kidney.

Histopathological Examination in ZP-induced Kidney Injury. To evaluate the tissue injury, histopathological examination of kidneys 24 h after ZP administration (150 mg/kg) was performed. Vacuoles and the denaturation and aggregation of eosinophilic materials were observed in the kidney of mice co-treated with ZP and inhibitors, although the histological abnormality was mild in mice receiving only ZP, and no abnormality was observed in mice receiving vehicles or inhibitors only (Fig. 4A). In the anti-MPO antibody staining, the number of MPO-positive cells was significantly higher in mice receiving TOTP, BSO and ZP compared to mice receiving only ZP. In contrast, the infiltration of mononuclear cells into the renal cells was not observed in mice receiving vehicles and inhibitors only (Figs. 4B and 4C).

Changes in mRNA Expression Levels in Immune-, Inflammation- and

DMD Fast Forward. Published on April 25, 2016 as DOI: 10.1124/dmd.116.069575
This article has not been copyedited and formatted. The final version may differ from this version.

Oxidative Stress-related Genes in Kidney. To investigate whether immune-, inflammation- and oxidative stress-related factors are involved in ZP-induced kidney injury, time-dependent changes in the renal mRNA expression levels of IL-1α, IL-6, MIP-2, ICAM-1, S100A9 and HO-1 were measured (Fig. 5). IL-1α mRNA expression levels in mice treated only with ZP were significantly increased 12 h after ZP administration. In mice treated with TOTP, BSO and ZP, the levels increased not only at 12 h but also 1 h after ZP administration. IL-6 and ICAM-1 mRNA expression levels in mice receiving TOTP, BSO and ZP were significantly increased in mice receiving TOTP, BSO and ZP 1 h and 12 h after ZP administration, in contrast to the small increase in mice receiving only ZP. S100A9 mRNA expression levels in mice that were treated only with ZP were significantly increased 1 h after ZP administration, but in TOTP, BSO and ZP-treated mice, the levels were significantly higher 12 h and 24 h after ZP administration. In only mice treated with only TOTP, BSO and ZP, the mRNA expression levels of HO-1 were significantly increased 12 h and 24 h after ZP administration. Although the mRNA expression levels of transcription factors for the Th lineage in adaptive immunity, such as the T-box expressed in T cells, GATA-binding domain-3 retinoid-related orphan receptor-γt and forkhead box P3, no change was observed in their expression between any groups (data not shown).

DMD Fast Forward. Published on April 25, 2016 as DOI: 10.1124/dmd.116.069575
This article has not been copyedited and formatted. The final version may differ from this version.

Involvement of Oxidative Stress in ZP-induced Kidney Injury. To confirm the depletion of GSH by BSO treatment and to investigate the involvement of oxidative stress in ZP-induced kidney injury, GSH and GSSG contents in kidney and liver were measured (Figs. 6A-6C). In the kidney, GSH depletion by BSO was confirmed in mice treated with TOTP and BSO. In addition, GSH levels in mice receiving TOTP, BSO and ZP were significantly lower compared to mice receiving only inhibitors. Owing to the decrease in GSH levels, the GSH/GSSG ratio, a biomarker of oxidative stress, was significantly lower in BSO, TOTP and ZP-treated mice compared to BSO and TOTP-treated mice. In the liver, GSH was depleted by BSO, but the GSH/GSSH ratio was not different between the TOTP and BSO-treated group and the TOTP, BSO and ZP-treated groups.

In addition, MDA concentrations, a biomarker of lipid peroxidation, were measured in the kidney and liver (Fig. 6D). In the kidney, MDA concentrations were significantly higher in TOTP, BSO and ZP-treated mice compared to TOTP and BSO-treated mice, but in the liver, there was no change in MDA concentrations between these groups.

Effect of Antioxidant Agents on ZP-induced Kidney Injury. The changes in oxidative stress markers implied the involvement of oxidative stress in ZP-induced

kidney injury. Next, the effect of tempol, an antioxidant agent, on ZP-induced kidney injury was investigated. The co-administration of tempol significantly decreased the plasma CRE levels at 12 h and the BUN levels at 12 and 24 h after ZP administration in BSO, TOTP and ZP-treated mice (Fig. 7). These results also support the involvement of oxidative stress in ZP-induced kidney injury.

DMD Fast Forward. Published on April 25, 2016 as DOI: 10.1124/dmd.116.069575
This article has not been copyedited and formatted. The final version may differ from this version.

Discussion

AGs of drugs are generally unstable and are believed to be involved in drug-induced toxicity via the formation of covalent adducts to endogenous proteins. Although there is increasing evidence that AGs form drug–protein adducts due to their chemical reactivity (Wang et al., 2001; Horng and Benet, 2013), cytotoxicity and genotoxicity of AGs have not been observed in vitro (Koga et al., 2011). Conversely, the AGs of warning and withdrawn drugs, such as zomepirac and diclofenac, induced the mRNA expression levels of immune- and inflammation-related genes in human PBMCs (Miyashita et al., 2014; Iwamura et al., 2015) Thus, these *in vitro* studies indicate that the toxicity of AGs remains controversial.

ZP is a nonsteroidal anti-inflammatory drug that was withdrawn from the market because of severe adverse effects, such as anaphylaxis and renal toxicity (Smith, 1982; Miller et al., 1983; Heintz, 1995). ZP-AG, a glucuronide conjugate metabolite of ZP, covalently binds proteins such as microtubular protein and dipeptidyl peptidase IV *in vitro* and *in vivo*, suggesting the involvement of ZP-AG in ZP-induced toxicity (Bailey et al., 1998; Wang et al., 2001). However, an animal model for the toxicity induced by ZP-AG has never been reported. To establish a mouse model of the toxicity induced by

ZP-AG, we attempted to increase the exposure to ZP-AG in mice by inhibiting its hydrolysis by using an esterase inhibitor. A previous study reported that ZP-AG is hydrolyzed by esterases (Smith et al., 1990b). TOTP, a non-selective esterase inhibitor, successfully inhibited esterase activity in mice and rats *in vivo* (Silver and Murphy, 1981; Kobayashi et al., 2012). In the present study, in addition to TOTP, BSO was used to reduce the GSH conjugation of ZP-AG.

Renal and hepatic toxicity was not observed after the administration of only ZP. Co-administration of TOTP significantly increased the plasma CRE and BUN levels and that of BSO moderately increased them. Co-administration of TOTP and BSO with ZP led to the severest renal toxicity, suggesting that hydrolysis and GSH conjugation of ZP-AG play a role in the detoxification of ZP-AG. In contrast to plasma CRE and BUN levels, plasma ALT levels were not elevated in any group, which corresponds to the fact that acute kidney injury was frequently reported in ZP therapy in humans (Smith, 1982; Miller et al., 1983). The present study succeeded in establishing an animal model of ZP-induced kidney injury by co-administration of TOTP and BSO.

To examine the relationship between the extent of kidney injury and the exposure to ZP and ZP-AG, the concentrations of ZP and ZP-AG in the plasma, kidney and liver were measured. ZP-AG concentrations in plasma, kidney and liver were significantly

higher in mice receiving TOTP, BSO and ZP compared to mice receiving ZP alone. The opposite changes in the levels of ZP and ZP-AG by TOTP and BSO treatment indicate that these inhibitors inhibit the hydrolysis of ZP-AG to ZP rather than the efflux of ZP-AG from kidney. A particularly high concentration of ZP-AG was observed in the kidney, suggesting that ZP-AG had the potential to lead to kidney injury. ZP-AG concentrations in the liver were much lower than those in the kidney, although the ZP concentrations in the liver were almost the same as those in the kidney. These results indicated that ZP-AG was more toxic than ZP because no hepatotoxicity was observed after ZP dosing. ZP and its metabolites are primarily excreted into the urine, and the urinary principal metabolite is ZP-AG in both mice and humans, although the urinary excretion ratio of ZP-AG in humans is higher than that in mice (57% and 19-28% of dose, respectively) (Grindel et al., 1980). The plasma concentration of ZP-AG in mice was approximately 50-fold higher than that in humans (100 mg/man, oral) corresponding to the ratio of dose (Smith et al., 1985b). In the present study, ZP-AG was highly accumulated in kidney, suggesting that ZP-AG was not equilibrated between plasma and kidney and might be actively transported to kidney. Moreover, the expression patterns of esterases and UGTs in kidney and other tissues were different between mice and humans (Paul and Fottrell, 1961; Oda et al., 2015). Therefore, further

investigations of interspecies differences in transporters, esterases and UGTs are needed. Of course, the uncertainty of interspecies sensitivity to toxicity should be also considered.

In general, glucuronides in hepatocytes are eliminated into the bile and blood mediated by multidrug-resistance protein (Mrp) 2 and Mrp 3, respectively (Trauner and Boyer, 2003). In human hepatocytes, the AGs of NSAIDs (diclofenac, naproxen, ketoprofen and ibuprofen) were rapidly excreted and did not accumulate in the cell (Koga et al., 2011). ZP-AG is immediately exported from the liver into blood rather than bile because excretion of ZP and its metabolites into bile is a minor route in humans and laboratory animals (Grindel et al., 1980). Thus, these reports support the finding that ZP-AG accumulated in the kidney but not in the liver.

In histopathological examination, our mouse model of ZP-induced kidney injury displayed vacuoles, denatured cytoplasm and aggregated eosinophilic materials, probably reflecting cellular necrosis. In ZP-induced kidney injury in the clinic, renal cortical necrosis was observed (Darwish et al., 1984). Thus, the results observed in the present study are consistent with the clinical findings. In preclinical studies, almost all of the NSAIDs produced papillary necrosis in experimental animal models (Whelton and Hamilton, 1991). A possible mechanism of papillary necrosis is ischemic injury

through the direct inhibition of cyclooxygenase-mediated production of prostaglandins (Brix, 2002). However, the inhibition of cyclooxygenase mediated by ZP might not contribute to ZP-induced kidney injury because papillary necrosis was not observed in this injury. The increased number of MPO-positive cells suggested the contribution of immune cell infiltration to ZP-induced kidney injury.

From our previous findings, AGs of warning and withdrawn drugs induced immune- and inflammation-related genes such as IL-6 and IL-8 in human PBMCs (Miyashita et al., 2014; Iwamura et al., 2015). Hence, the changes in the renal mRNA expression levels of immune- and inflammation-related genes were measured. The mRNA expression of IL-1α and IL-6 were induced in mice highly exposed to ZP-AG, followed by ICAM-1 and S100A9 mRNAs. IL-1α, a trigger of chemokine cascades, other cytokines and inflammatory mediators, is synthesized in the first few hours after injury or the ischemic event (Dinarello et al., 2012). IL-6 is also rapidly induced as a lymphocyte-stimulating factor and leads to innate and adaptive immune activation (Hunter and Jones, 2015). ICAM-1, an adhesion molecule, is involved in infiltration of inflammatory cells (Ley et al., 2007). S100A9, a damage-associated molecular pattern (DAMP), is released from activated or necrotic neutrophils and monocytes/macrophages and promotes innate immune and inflammation (Schiopu and Cotoi, 2013) The

stimulation of IL-1α induces ICAM-1 and S100A9 (Aziz and Wakefield, 1996; Zreiqat et al., 2010), and so does IL-6 (Wung et al., 2005; Lee et al., 2012). Because the injection of recombinant IL-1α accelerates renal injury and mortality in mice (Brennan et al., 1989), and IL-6- or ICAM-1-deficient mice show protective effects against acute kidney injury, these factors could trigger and promote kidney injury (Kelly et al., 1996; Nechemia-Arbely et al., 2008). Taken together, it is conceivable that IL-1α and IL-6 induced by ZP-AG at the onset promoted the infiltration of immune cells via the induction of ICAM-1 and MIP-2, and then the infiltrating cells caused kidney injury.

Of particular note was the potent induction of HO-1 mRNA in mice co-treated with TOTP and BSO, suggesting that ZP-AG was involved in ZP-induced kidney injury via the induction of oxidative stress. The decrease in the GSH/GSSG ratio and the increase in MDA concentration were observed in the kidney, but not in the liver, consistent with each tissue injury. Partial involvement of oxidative stress was also demonstrated by tempol treatment. In accordance with the results of the GSH/GSSG ratio and the MDA concentration, the antioxidant tempol suppressed ZP-induced kidney injury, suggesting that oxidative stress is involved in renal toxicity. It was reported that the decrease in the GSH/GSSG ratio and the increase in the MDA concentrations were also observed in cisplatin-induced acute renal failure in rats (Santos et al., 2007).

Tempol attenuated oxidative stress-mediated renal injury in rats (Chatterjee et al., 2000). These results were similar to the results observed in the present study.

In conclusion, a mouse model for ZP-induced kidney injury was established by using TOTP and BSO in consideration of the metabolic pathway of ZP. From the pharmacokinetics of ZP and ZP-AG, it was shown that the hydrolysis of ZP-AG by esterases contributed considerably to their pharmacokinetics and ZP-AG could be responsible for ZP-induced kidney injury *in vivo*. In addition, it was demonstrated that the renal toxicity was mediated via oxidative stress and immune cell infiltration (Fig. 8). The model using TOTP can be used to evaluate the toxicity of AGs in preclinical settings, and the present study sheds light on understanding the toxicological potential of AGs.

Acknowledgment

We greatly appreciate the valuable suggestions of Professor Miki Nakajima.

DMD Fast Forward. Published on April 25, 2016 as DOI: 10.1124/dmd.116.069575
This article has not been copyedited and formatted. The final version may differ from this version.

Authorship contributions

Participated in research design: Iwamura, Yokoi.

Conducted experiments: Iwamura, Watanabe, Akai, Nishinosono, Tsuneyama.

Contributed new reagents or analytic tools: Iwamura, Watanabe, Nishinosono.

Performed data analysis: Iwamura, Watanabe, Tsuneyama.

Wrote or contributed to the writing of the manuscript: Iwamura, Oda, Yokoi, Kume.

References

Aziz KE and Wakefield D (1996) Modulation of endothelial cell expression of ICAM-1, E-selectin, and VCAM-1 by β-estradiol, progesterone, and dexamethasone. *Cell Immunol* **167:**79-85.

Bailey MJ and Dickinson RG (2003) Acyl glucuronide reactivity in perspective: biological consequences. *Chem Biol Interact* **145:**117-137.

Bailey MJ, Worrall S, de Jersey J, and Dickinson RG (1998) Zomepirac acyl glucuronide covalently modifies tubulin in vitro and in vivo and inhibits its assembly in an in vitro system. *Chem Biol Interact* **115:**153-166.

Benet LZ, Spahn-Langguth H, Iwakawa S, Volland C, Mizuma T, Mayer S, Mutschler E, and Lin ET (1993) Predictability of the covalent binding of acidic drugs in man. *Life Sci* **53:**PL141-146.

Boelsterli UA (2002) Xenobiotic acyl glucuronides and acyl CoA thioesters as protein-reactive metabolites with the potential to cause idiosyncratic drug reactions. *Curr Drug Metab* **3:**439-450.

Brennan DC, Yui MA, Wuthrich RP, and Kelley VE (1989) Tumor necrosis factor and IL-1 in New Zealand Black/White mice. Enhanced gene expression and acceleration of renal injury. *J Immunol* **143:**3470-3475.

Brix AE (2002) Renal papillary necrosis. *Toxicol Pathol* **30:**672-674.

Chatterjee PK, Cuzzocrea S, Brown PA, Zacharowski K, Stewart KN, Mota-Filipe H, and Thiemermann C (2000) Tempol, a membrane-permeable radical scavenger, reduces oxidant stress-mediated renal dysfunction and injury in the rat. *Kidney Int* **58:**658-673.

Darnell M, Breitholtz K, Isin EM, Jurva U, and Weidolf L (2015) Significantly Different Covalent Binding of Oxidative Metabolites, Acyl Glucuronides, and S-Acyl CoA Conjugates Formed from Xenobiotic Carboxylic Acids in Human Liver Microsomes. *Chem Res Toxicol* **28:**886-896.

Darwish R, Vaziri ND, Gupta S, Novey H, Spear GS, Licorish K, Powers D, and Cesario T (1984) Focal renal cortical necrosis associated with zomepirac. *Am J Med* **76:**1113-1117.

Dinarello CA, Simon A, and van der Meer JW (2012) Treating inflammation by blocking interleukin-1 in a broad spectrum of diseases. *Nat Rev Drug Discov* **11:**633-652.

Emeigh Hart SG, Beierschmitt WP, Bartolone JB, Wyand DS, Khairallah EA, and Cohen SD (1991) Evidence against deacetylation and for cytochrome P450-mediated activation in acetaminophen-induced nephrotoxicity in the CD-1

mouse. *Toxicol Appl Pharmacol* **107:**1-15.

Faed EM (1984) Properties of acyl glucuronides: implications for studies of the pharmacokinetics and metabolism of acidic drugs. *Drug Metab Rev* **15:**1213-1249.

Griffith OW (1980) Determination of glutathione and glutathione disulfide using glutathione reductase and 2-vinylpyridine. *Anal Biochem* **106:**207-212.

Grillo MP and Hua F (2003) Identification of zomepirac-S-acyl-glutathione in vitro in incubations with rat hepatocytes and in vivo in rat bile. *Drug Metab Dispos* **31:**1429-1436.

Grindel JM, O'Neill PJ, Yorgey KA, Schwartz MH, McKown LA, Migdalof BH, and Wu WN (1980) The metabolism of zomepirac sodium. I. Disposition in laboratory animals and man. *Drug Metab Dispos* **8:**343-348.

Heintz RC (1995) Tenoxicam and renal function. *Drug Saf* **12:**110-119.

Horng H and Benet LZ (2013) The nonenzymatic reactivity of the acyl-linked metabolites of mefenamic acid toward amino and thiol functional group bionucleophiles. *Drug Metab Dispos* **41:**1923-1933.

Hunter CA and Jones SA (2015) IL-6 as a keystone cytokine in health and disease. *Nat Immunol* **16:**448-457.

Iwamura A, Fukami T, Higuchi R, Nakajima M, and Yokoi T (2012) Human α/β hydrolase domain containing 10 (ABHD10) is responsible enzyme for deglucuronidation of mycophenolic acid acyl-glucuronide in liver. *J Biol Chem* **287:**9240-9249.

Iwamura A, Ito M, Mitsui H, Hasegawa J, Kosaka K, Kino I, Tsuda M, Nakajima M, Yokoi T, and Kume T (2015) Toxicological evaluation of acyl glucuronides utilizing half-lives, peptide adducts, and immunostimulation assays. *Toxicol In Vitro.*

Jinno N, Ohashi S, Tagashira M, Kohira T, and Yamada S (2013) A simple method to evaluate reactivity of acylglucuronides optimized for early stage drug discovery. *Biol Pharm Bull* **36:**1509-1513.

Kelly KJ, Williams WW, Jr., Colvin RB, Meehan SM, Springer TA, Gutierrez-Ramos JC, and Bonventre JV (1996) Intercellular adhesion molecule-1-deficient mice are protected against ischemic renal injury. *J Clin Invest* **97:**1056-1063.

Kobayashi Y, Fukami T, Higuchi R, Nakajima M, and Yokoi T (2012) Metabolic activation by human arylacetamide deacetylase, CYP2E1, and CYP1A2 causes phenacetin-induced methemoglobinemia. *Biochem Pharmacol* **84:**1196-1206.

Koga T, Fujiwara R, Nakajima M, and Yokoi T (2011) Toxicological evaluation of acyl

glucuronides of nonsteroidal anti-inflammatory drugs using human embryonic kidney 293 cells stably expressing human UDP-glucuronosyltransferase and human hepatocytes. *Drug Metab Dispos* **39:**54-60.

Kumada T, Tsuneyama K, Hatta H, Ishizawa S, and Takano Y (2004) Improved 1-h rapid immunostaining method using intermittent microwave irradiation: practicability based on 5 years application in Toyama Medical and Pharmaceutical University Hospital. *Mod Pathol* **17:**1141-1149.

Lee MJ, Lee JK, Choi JW, Lee CS, Sim JH, Cho CH, Lee KH, Cho IH, Chung MH, Kim HR, and Ye SK (2012) Interleukin-6 induces S100A9 expression in colonic epithelial cells through STAT3 activation in experimental ulcerative colitis. *PLoS One* **7:**e38801.

Ley K, Laudanna C, Cybulsky MI, and Nourshargh S (2007) Getting to the site of inflammation: the leukocyte adhesion cascade updated. *Nat Rev Immunol* **7:**678-689.

Miller FC, Schorr WJ, and Lacher JW (1983) Zomepirac-induced renal failure. *Arch Intern Med* **143:**1171-1173.

Miyashita T, Kimura K, Fukami T, Nakajima M, and Yokoi T (2014) Evaluation and mechanistic analysis of the cytotoxicity of the acyl glucuronide of nonsteroidal

anti-inflammatory drugs. *Drug Metab Dispos* **42:**1-8.

Nechemia-Arbely Y, Barkan D, Pizov G, Shriki A, Rose-John S, Galun E, and Axelrod JH (2008) IL-6/IL-6R axis plays a critical role in acute kidney injury. *J Am Soc Nephrol* **19:**1106-1115.

Oda S, Fukami T, Yokoi T, and Nakajima M (2015) A comprehensive review of UDP-glucuronosyltransferase and esterases for drug development. *Drug Metab Pharmacokinet* **30:**30-51.

O'Neill PJ, Yorgey KA, Renzi NL, Jr., Williams RL, and Benet LZ (1982) Disposition of zomepirac sodium in man. *J Clin Pharmacol* **22:**470-476.

Paul J and Fottrell P (1961) Tissue-specific and species-specific esterases. *Biochem J* **78:**418-424.

Santos NA, Catao CS, Martins NM, Curti C, Bianchi ML, and Santos AC (2007) Cisplatin-induced nephrotoxicity is associated with oxidative stress, redox state unbalance, impairment of energetic metabolism and apoptosis in rat kidney mitochondria. *Arch Toxicol* **81:**495-504.

Sawamura R, Okudaira N, Watanabe K, Murai T, Kobayashi Y, Tachibana M, Ohnuki T, Masuda K, Honma H, Kurihara A, and Okazaki O (2010) Predictability of idiosyncratic drug toxicity risk for carboxylic acid-containing drugs based on the

chemical stability of acyl glucuronide. *Drug Metab Dispos* **38:**1857-1864.

Schiopu A and Cotoi OS (2013) S100A8 and S100A9: DAMPs at the crossroads between innate immunity, traditional risk factors, and cardiovascular disease. *Mediators Inflamm* **2013:**828354.

Shimizu S, Atsumi R, Itokawa K, Iwasaki M, Aoki T, Ono C, Izumi T, Sudo K, and Okazaki O (2009) Metabolism-dependent hepatotoxicity of amodiaquine in glutathione-depleted mice. *Arch Toxicol* **83:**701-707.

Silver EH and Murphy SD (1981) Potentiation of acrylate ester toxicity by prior treatment with the carboxylesterase inhibitor triorthotolyl phosphate (TOTP). *Toxicol Appl Pharmacol* **57:**208-219.

Smith PC, Hasegawa J, Langendijk PN, and Benet LZ (1985a) Stability of acyl glucuronides in blood, plasma, and urine: studies with zomepirac. *Drug Metab Dispos* **13**:110-112.

Smith PC, Langendijk PN, Bosso JA, and Benet LZ (1985b) Effect of probenecid on the formation and elimination of acyl glucuronides: studies with zomepirac. *Clin Pharmacol Ther* **38**:121-127.

Smith PC, Benet LZ, and McDonagh AF (1990a) Covalent binding of zomepirac glucuronide to proteins: evidence for a Schiff base mechanism. *Drug Metab*

Dispos **18:**639-644.

Smith PC, McDonagh AF, and Benet LZ (1990b) Effect of esterase inhibition on the disposition of zomepirac glucuronide and its covalent binding to plasma proteins in the guinea pig. *J Pharmacol Exp Ther* **252:**218-224.

Smith VT (1982) Anaphylactic shock, acute renal failure, and disseminated intravascular coagulation. Suspected complications of zomepirac. *JAMA* **247:**1172-1173.

Suzuki E, Yamamura N, Ogura Y, Nakai D, Kubota K, Kobayashi N, Miura S, and Okazaki O (2010) Identification of valproic acid glucuronide hydrolase as a key enzyme for the interaction of valproic acid with carbapenem antibiotics. *Drug Metab Dispos* **38:**1538-1544.

Tietze F (1969) Enzymic method for quantitative determination of nanogram amounts of total and oxidized glutathione: applications to mammalian blood and other tissues. *Anal Biochem* **27:**502-522.

Trauner M and Boyer JL (2003) Bile salt transporters: molecular characterization, function, and regulation. *Physiol Rev* **83:**633-671.

Wang J, Davis M, Li F, Azam F, Scatina J, and Talaat R (2004) A novel approach for predicting acyl glucuronide reactivity via Schiff base formation: development of

rapidly formed peptide adducts for LC/MS/MS measurements. *Chem Res Toxicol* **17:**1206-1216.

Wang M, Gorrell MD, McGaughan GW, and Dickinson RG (2001) Dipeptidyl peptidase IV is a target for covalent adduct formation with the acyl glucuronide metabolite of the anti-inflammatory drug zomepirac. *Life Sci* **68:**785-797.

Whelton A and Hamilton CW (1991) Nonsteroidal anti-inflammatory drugs: effects on kidney function. *J Clin Pharmacol* **31:**588-598.

Wung BS, Ni CW, and Wang DL (2005) ICAM-1 induction by TNFα and IL-6 is mediated by distinct pathways via Rac in endothelial cells. *J Biomed Sci* **12:**91-101.

Zreiqat H, Belluoccio D, Smith MM, Wilson R, Rowley LA, Jones K, Ramaswamy Y, Vogl T, Roth J, Bateman JF, and Little CB (2010) S100A8 and S100A9 in experimental osteoarthritis. *Arthritis Res Ther* **12:**R16.

Footnotes

Send reprint requests to: Atsushi Iwamura, DMPK Research Laboratory, Mitsubishi Tanabe Pharma Corporation, 2-2-50 Kawagishi, Toda, Saitama 335-8505, Japan

E-mail: Iwamura.Atsushi@mf.mt-pharma.co.jp

DMD Fast Forward. Published on April 25, 2016 as DOI: 10.1124/dmd.116.069575
This article has not been copyedited and formatted. The final version may differ from this version.

Figure Legends.

Fig. 1. Changes in plasma CRE (A), BUN (B) and ALT (C) levels in female BALB/c mice after ZP administration. TOTP (50 mg/kg in corn oil, p.o.), BSO (700 mg/kg in saline, i.p.) and ZP (150 mg/kg in KPB, i.p.) were administered as described in Materials and Methods. The plasma CRE, BUN and ALT levels were measured 24 h after ZP administration. The data are shown as the mean ± S.E.M. (n = 5-7). The statistical analyses were performed using one-way ANOVA followed by Dunnett's test. ***P* < 0.01 compared with the vehicles (corn oil, saline and KPB)-treated group. #*P* < 0.05, ##*P* < 0.01 compared with only ZP-treated group.

Fig. 2. Dose-dependent changes in plasma CRE (A), BUN (B) and ALT (C) levels after ZP administration in mice. TOTP and BSO were administered as described in Materials and Methods. ZP was administered at a dose of 50, 100 and 150 mg/kg. The plasma CRE, BUN and ALT levels were measured 24 h after ZP administration. The data are shown as the mean ± S.E.M. (n = 5-7). Differences compared with only inhibitors-treated group were considered significant at **P* < 0.05, ***P* < 0.01 one-way ANOVA followed by Dunnett's test.

DMD Fast Forward. Published on April 25, 2016 as DOI: 10.1124/dmd.116.069575
This article has not been copyedited and formatted. The final version may differ from this version.

Fig. 3. Time-dependent changes in plasma CRE (A), BUN (B), ALT (C) levels and concentrations of ZP (D) and ZP-AG (E) in plasma, kidney and liver after ZP administration. TOTP, BSO and ZP were administered as described in Materials and Methods. The plasma CRE, BUN and ALT levels were measured 3, 6, 12 and 24 h after ZP administration. Concentrations of ZP and ZP-AG in plasma, kidney and liver were measured 0.5, 1, 3, 6, 12 and 24 h after ZP administration. The data are shown as the mean ± S.E.M. (n = 5-7). Differences in plasma CRE, BUN and ALT levels compared with only ZP-treated group were considered significant at $*P < 0.05$, $**P < 0.01$, $***P < 0.001$ by Student's *t*-tests. Differences in concentrations of ZP and ZP-AG in plasma, kidney and liver compared with only ZP-treated group were considered significant at $\#P < 0.05$ by Student's *t*-tests.

Fig. 4. Histopathological examination of mouse kidney after ZP administration. TOTP, BSO and ZP were administered as described in Materials and Methods. The kidneys were collected at 24 h after ZP administration, and the kidney sections were stained with hematoxylin and eosin (H&E) (A) or immunostained with an anti-myeloperoxidase (MPO) antibody (B). Arrowheads indicate immune cell infiltration. The number of

MPO-positive cells was counted and compared with only ZP-treated group (C). The data are shown as the mean ± S.E.M. (n = 5-7). The difference between only ZP-treated group and ZP and inhibitors-treated group was considered significant at $*P < 0.05$ by Student's *t*-tests.

Fig. 5. Time-dependent changes in the renal mRNA expression levels of immune-, inflammation- and oxidative stress-related genes in mice after ZP administration. TOTP, BSO and ZP were administered as described in Materials and Methods. The kidneys were collected at 1, 12 and 24 h after ZP administration. The expression level of each mRNA was measured by real-time RT-PCR and normalized to Gapdh mRNA as described in Materials and Methods. The data are shown as the mean ± S.E.M. (n = 5-6). The statistical analyses were performed using one-way ANOVA followed by Tukey's test. $*P < 0.05$, $**P < 0.01$, $***P < 0.001$, compared with only inhibitors-treated group. $\#P < 0.05$, $\#\#P < 0.01$, $\#\#\#P < 0.001$, compared with only ZP-treated group.

Fig. 6. The GSH (A) and GSSG (B) levels, GSH/GSSG ratio (C) and MDA levels (D) in kidney and liver after ZP administration. TOTP, BSO and ZP were administered as described in Materials and Methods. The kidney and liver were collected at 12 h after

ZP administration. The data are shown as the mean ± S.E.M. (n = 5-6). The difference between only inhibitors-treated group and ZP and inhibitors-treated group was considered significant at $^{**}P < 0.01$, $^{***}P < 0.001$ by Student's *t*-tests.

Fig. 7. Effect of an antioxidant agent in kidney injury of ZP-administered mice. TOTP, BSO, ZP and tempol were administered as described in Materials and Methods. The plasma CRE (A) and BUN (B) levels were measured 12 and 24 h after ZP administration. The data are shown as the mean ± S.E.M. (n = 6). Differences compared to the no tempol-treated group were considered significant at $^{*}P < 0.05$, $^{***}P < 0.001$ by Student's *t*-tests.

Fig. 8. Proposed mechanisms of kidney injury induced by ZP-AG.

DMD Fast Forward. Published on April 25, 2016 as DOI: 10.1124/dmd.116.069575
This article has not been copyedited and formatted. The final version may differ from this version.

TABLE 1

Sequences of primers used for real-time RT-PCR analyses

Genes		Primer sequences	NCBI accession No.
IL-1α	S	5'- TTACAGTGAAAACGAAGAC -3'	NM_010554.4
	AS	5'- GATCTGTGCAAGTCTCATGAAG -3'	
IL-6	S	5'- CCATAGCTACCTGGAGTACA -3'	NM_031168.1
	AS	5'- GGAAATTGGGGTAGGAAGGA -3'	
MIP-2	S	5'- AAGTTTGCCTTGACCCTGAAG -3'	NM_009140.2
	AS	5'- ATCAGGTACGATCCAGGCTTC -3'	
ICAM-1	S	5'- GCTACCATCACCGTGTATTCG -3'	NM_010493.2
	AS	5'- TGAGGTCCTTGCCTACTTGC -3'	
S100A9	S	5'- GATGGCCAACAAAGCACCTT -3'	NM_009114.3
	AS	5'- CCTCAAAGCTCAGCTGATTG -3'	
HO-1	S	5'- GACACCTGAGGTCAAGCACA -3'	NM_010442.2
	AS	5'- ATCACCTGCAGCTCCTCAAA -3'	

S, Sense; AS, Anti-sense.

IL, interleukin; MIP-2, macrophage inflammatory protein-2; ICAM-1, intercellular adhesion molecule-1; S100A9, S100 calcium-binding protein A9; HO-1, heme oxygenase 1.

Figure 1

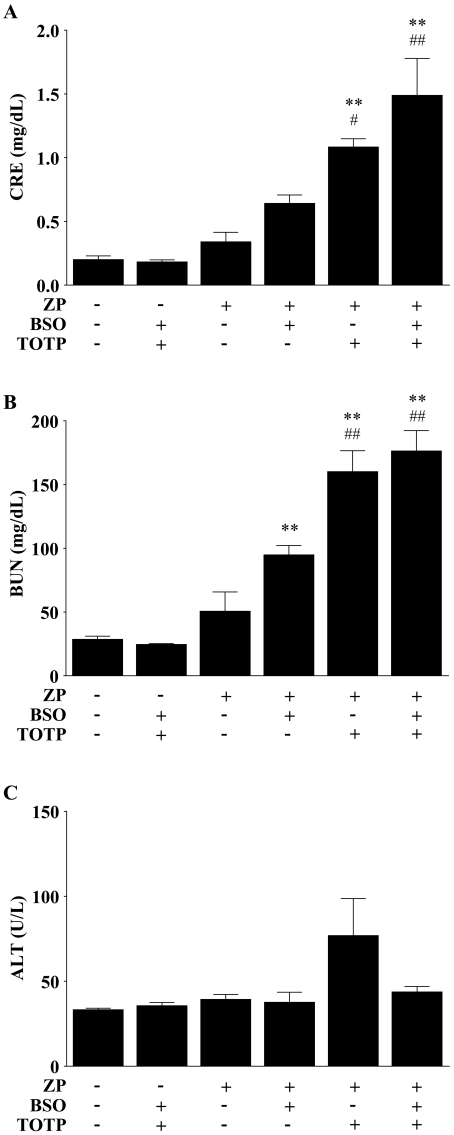
A
CRE (mg/dL)
2.0
1.5
1.0
0.5
0.0
** #
** ##
ZP - - + + + +
BSO - + - + - +
TOTP - + - - + +
B
BUN (mg/dL)
200
150
100
50
0
**
** ##
** ##
ZP - - + + + +
BSO - + - + - +
TOTP - + - - + +
C
ALT (U/L)
150
100
50
0
ZP - - + + + +
BSO - + - + - +
TOTP - + - - + +

Figure 2

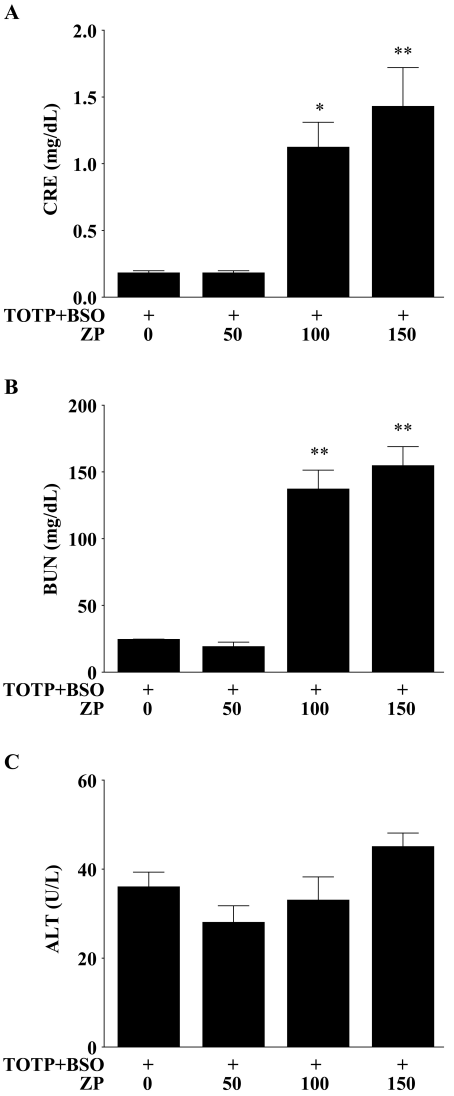
A
2.0
1.5
1.0
0.5
0.0
CRE (mg/dL)
*
**
TOTP+BSO + + + +
ZP 0 50 100 150
B
200
150
100
50
0
BUN (mg/dL)
**
**
TOTP+BSO + + + +
ZP 0 50 100 150
C
60
40
20
0
ALT (U/L)
TOTP+BSO + + + +
ZP 0 50 100 150

Figure 3

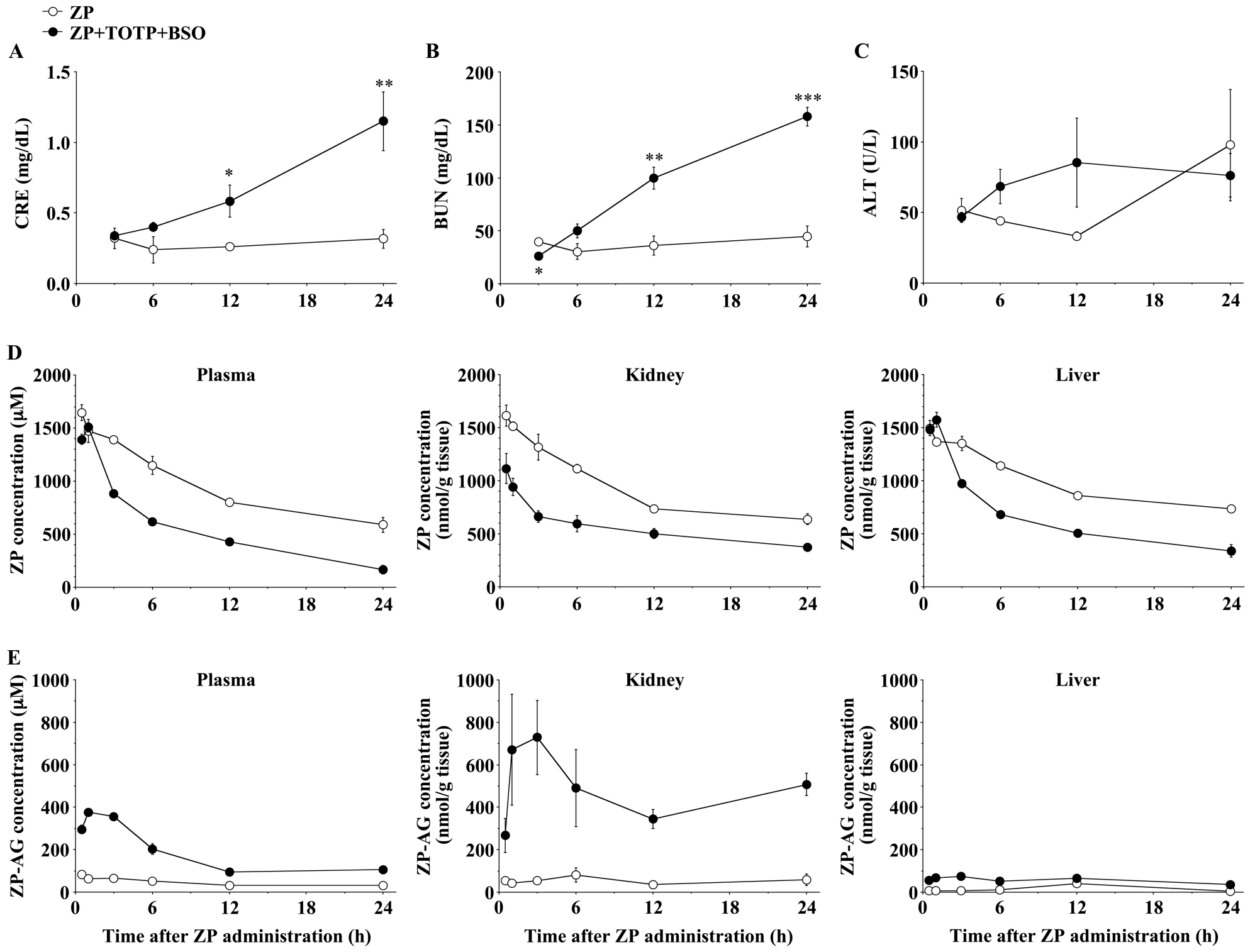
ZP
ZP+TOTP+BSO
A
CRE (mg/dL)
B
BUN (mg/dL)
C
ALT (U/L)
D
Plasma
Kidney
Liver
ZP concentration (μM)
ZP concentration (nmol/g tissue)
E
ZP-AG concentration (μM)
ZP-AG concentration (nmol/g tissue)
Time after ZP administration (h)

Figure 4

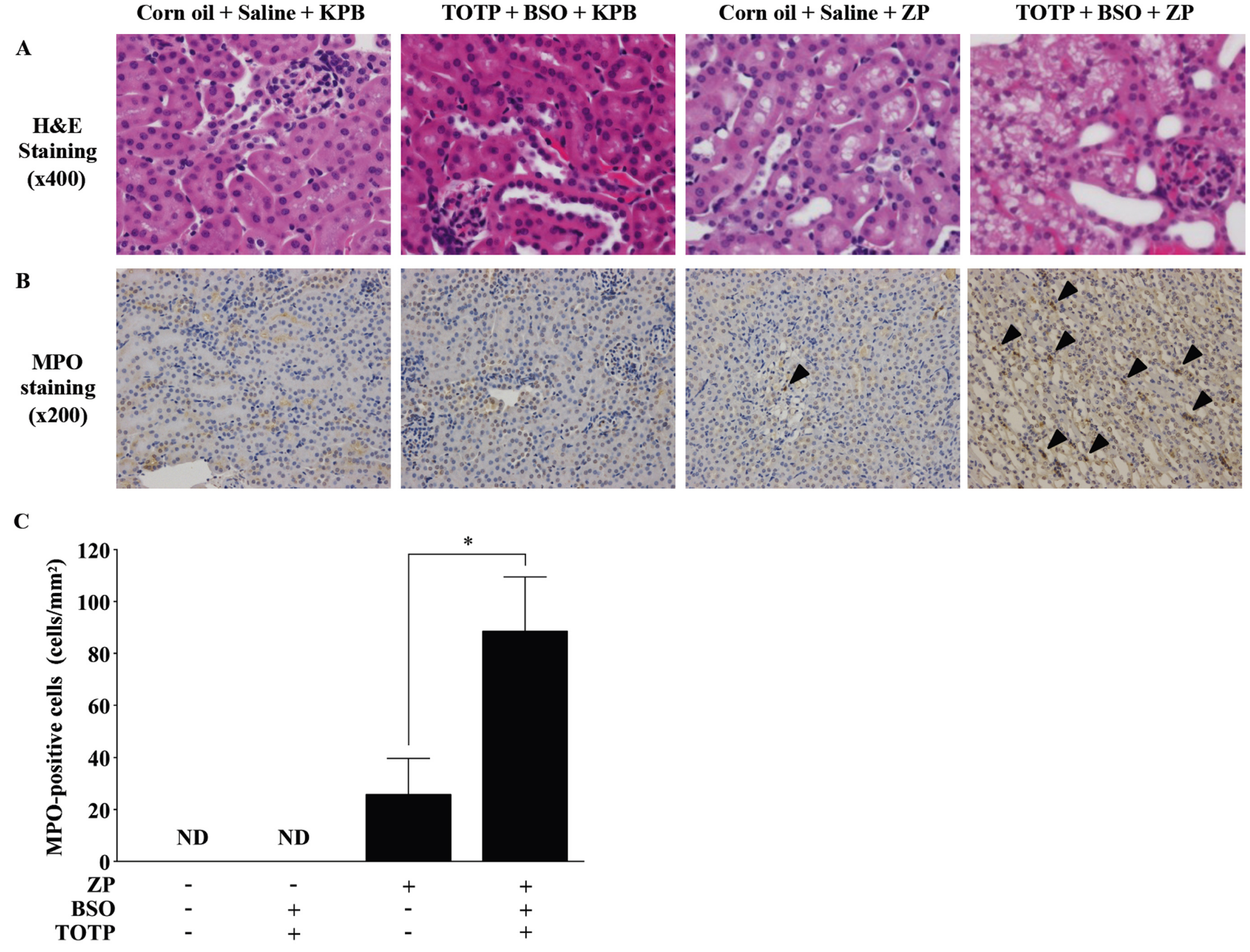
Corn oil + Saline + KPB
TOTP + BSO + KPB
Corn oil + Saline + ZP
TOTP + BSO + ZP
A
H&E Staining (x400)
B
MPO staining (x200)
C
MPO-positive cells (cells/mm²)
120
100
80
60
40
20
0
*
ND
ND
ZP - - + +
BSO - + - +
TOTP - + - +

Figure 5

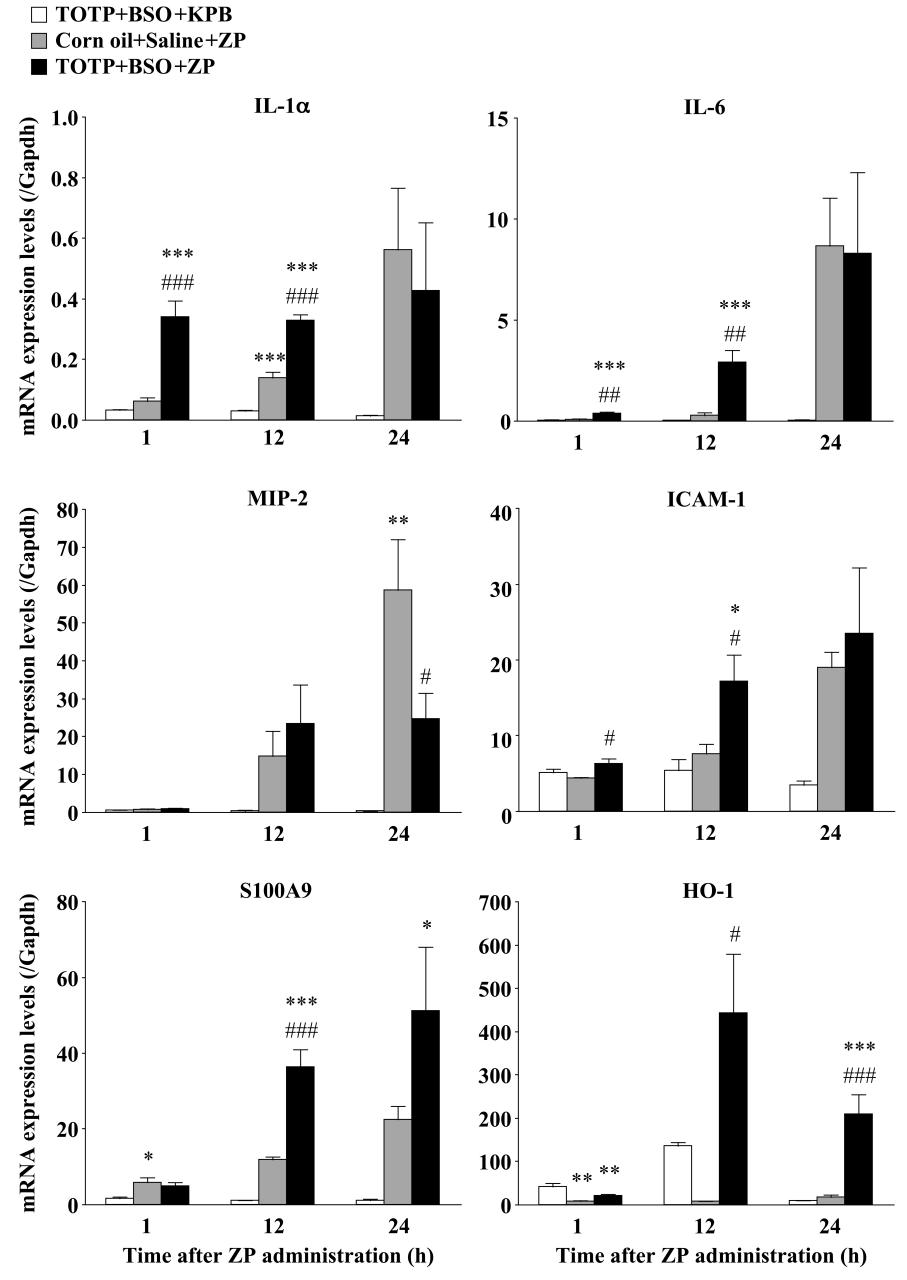
TOTP+BSO+KPB
Corn oil+Saline+ZP
TOTP+BSO+ZP
IL-1α
IL-6
MIP-2
ICAM-1
S100A9
HO-1
mRNA expression levels (/Gapdh)
Time after ZP administration (h)
1
12
24

Figure 6

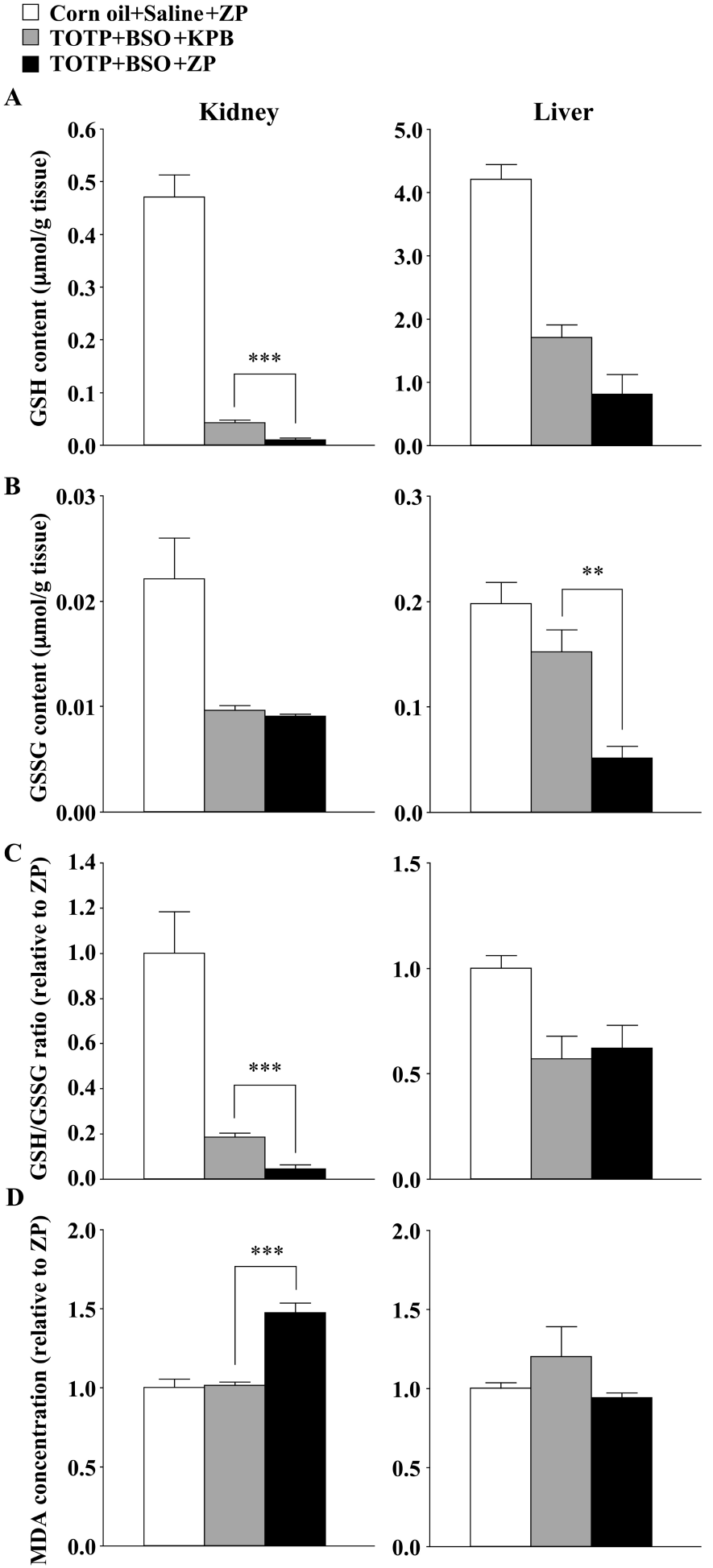
Corn oil+Saline+ZP
TOTP+BSO+KPB
TOTP+BSO+ZP
A
Kidney
Liver
GSH content (μmol/g tissue)
0.6
0.5
0.4
0.3
0.2
0.1
0.0
***
5.0
4.0
3.0
2.0
1.0
0.0
B
GSSG content (μmol/g tissue)
0.03
0.02
0.01
0.00
0.3
0.2
0.1
0.0
**
C
GSH/GSSG ratio (relative to ZP)
1.4
1.2
1.0
0.8
0.6
0.4
0.2
0.0
***
1.5
1.0
0.5
0.0
D
MDA concentration (relative to ZP)
2.0
1.5
1.0
0.5
0.0
***
2.0
1.5
1.0
0.5
0.0

Figure 7

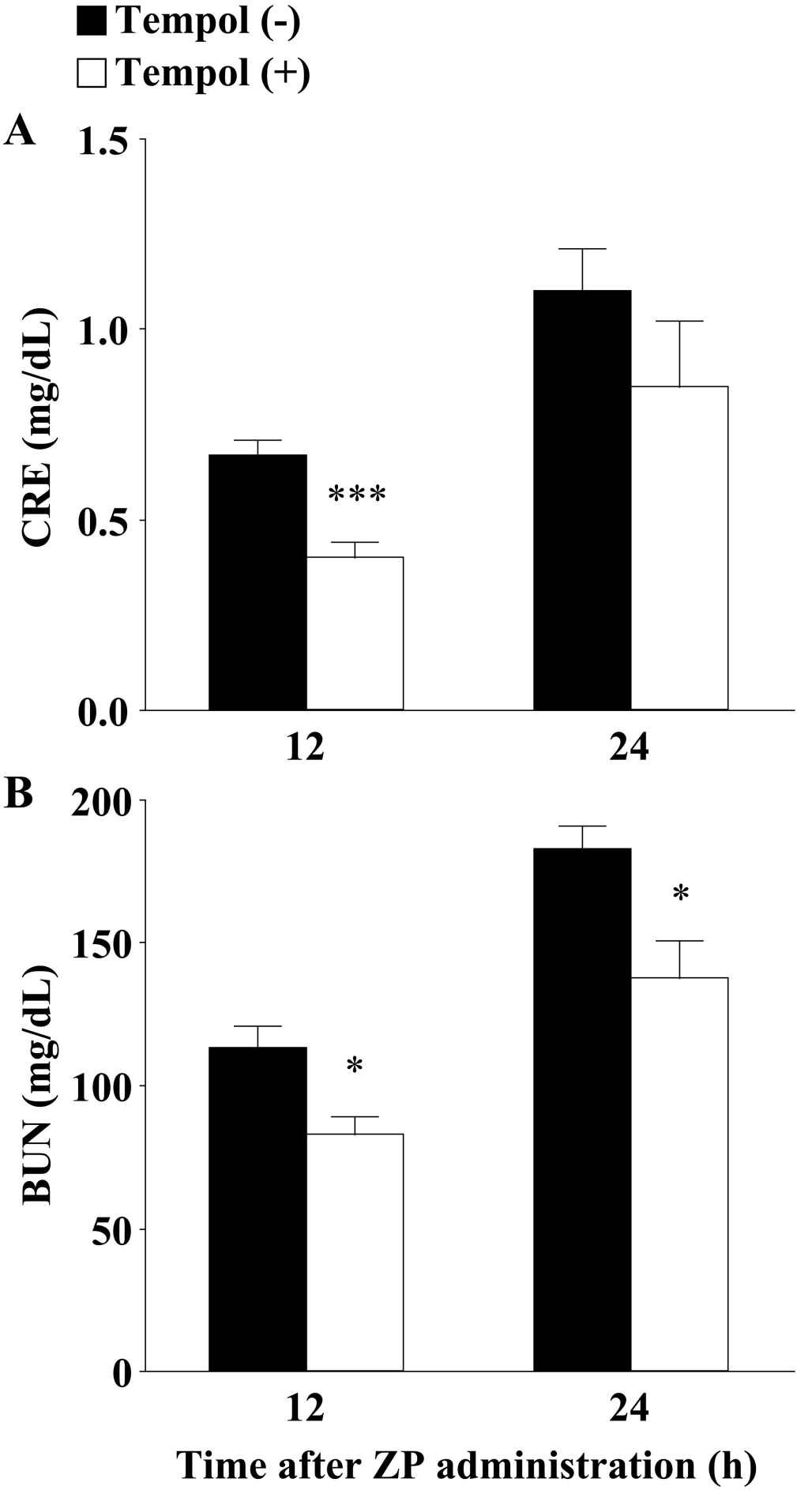
Tempol (-)
Tempol (+)
A
1.5
1.0
0.5
0.0
CRE (mg/dL)
***
12
24
B
200
150
100
50
0
BUN (mg/dL)
*
*
12
24
Time after ZP administration (h)

Figure 8

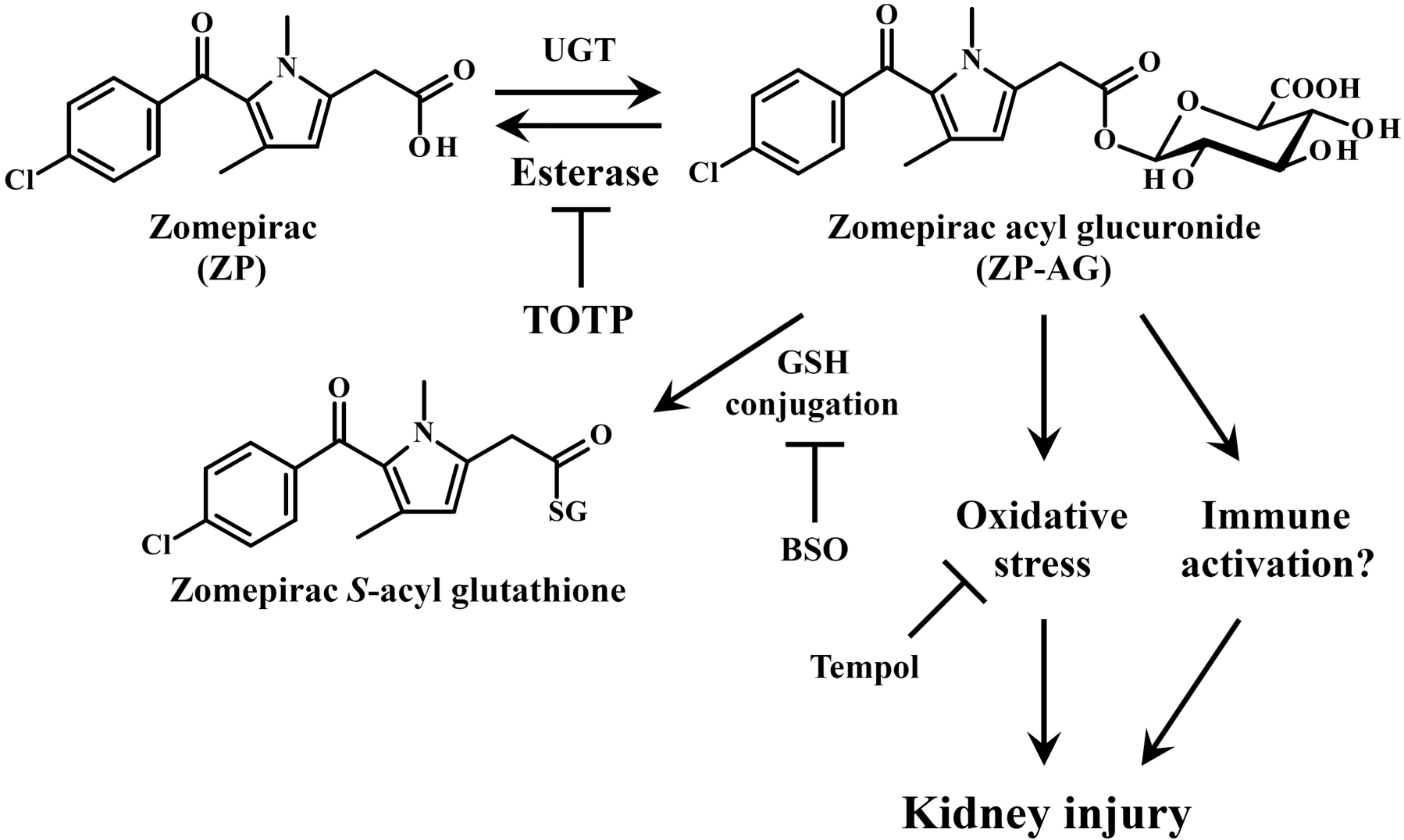
UGT
Esterase
TOTP
Zomepirac
(ZP)
Zomepirac acyl glucuronide
(ZP-AG)
GSH
conjugation
BSO
Zomepirac S-acyl glutathione
Oxidative
stress
Immune
activation?
Tempol
Kidney injury